Environ. Sci. Technol. **1998**, *32,* 2124−2129

Reactivity-Adjusted VOC Measurements by Airtrak: A Feasibility Study

TAI Y. CHANG,* MICHAEL D. HURLEY, BARBARA I. NANCE, AND STEVEN M. JAPAR*

Ford Research Laboratory, Ford Motor Company, MD-3083, P.O. Box 2053, Dearborn, Michigan 48121

Measurements of ozone precursors are essential to the understanding of ozone−precursor relationships in urban and rural areas. The feasibility of carrying out reactivity-adjusted VOC measurements using the Airtrak instrument has been investigated by modeling simulations and experiments. To quantitatively relate VOC to an ambient measurement of SP (smog produced), SP−VOC relationships have been derived by simulating flow-mode experiments performed using an Airtrak instrument. It has been found that, when the airstream contains only VOC and NO and the NO concentration is constant, the relationship between SP and VOC concentrations can be represented by a quadratic polynomial. This has been demonstrated both by flow-mode experiments and through model simulations. Because the response time in the photolytic chamber is approximately 30 min, any fine structure in the VOC concentrations is smoothed out, but time-averaged (e.g., 1 h average) concentrations agree well with inlet concentrations. To apply this methodology to the measurements of reactivity-adjusted VOC concentrations in ambient air samples, ozone and NO_2 have to be removed from air sample streams before VOC measurements are made, and the NO concentration in the Airtrak reactor has to be constant. NO concentration in the reactor can be maintained at a constant level by feedback control, and efficient scrubbers for ozone and NO_2 are available.

Introduction

Measurements of the concentrations of ozone precursors, volatile organic compounds (VOC) and NO_x ($NO + NO_2$), are essential to the understanding of ozone−precursor relationships in urban and regional areas. In the last two decades, major advances in measuring VOC and NO_x have been made. Reliable techniques for measuring NO_x are available currently, although it remains difficult to measure NO_2 without interference at routine monitoring sites (*1*). For VOC, reliable techniques are available for lighter nonmethane hydrocarbons (NMHC), while current techniques for measuring heavier NMHC and partially oxidized NMHC, including carbonyl compounds, are somewhat uncertain and are under continuing development (*1*). The standard approach for measurement of NMHC is based on gas chromatography−flame ionization detection (GC−FID), while other techniques are used for measurement of carbonyl and other compounds. More recently, automated GC systems have been employed to measure NMHC and oxygenated hydrocarbons [e.g., see Goldan et al. (*2*)]. However, these measurement techniques are time-consuming and expensive and can miss a significant fraction of VOC. Consequently, a simple measurement technique for reactivity-adjusted, total VOC would be valuable for evaluating ozone−precursor relationships.

The initial attempt at developing such a monitoring was reported (*3*) in 1956, and an improved ozone−precursor monitor, based on the early technology, has recently been discussed (*4, 5*). The latter ozone−precursor monitor used a discrete sample approach in which the sampled ambient air was irradiated in the reaction chamber with UV light for 10 min and the difference in ozone concentrations between ambient and 10-min irradiated air was used as a measure of the photochemical reactivity potential of the precursor blend in the sampled air. No attempt was made to derive VOC concentrations.

More recently, an integrated air quality assessment instrument, Airtrak, has been introduced (*6*). On the basis of the integrated empirical rate (IER) model of photochemical smog formation (*7*), the instrument, consisting of matched dark and photolytic flow reactors, is advertised to continuously measure smog formation coefficients and (albeit indirectly) reactivity-adjusted VOC concentrations in the sampled air.

Since there is some concern about the rigor of the IER model (*8, 9*), it is the purpose of the present paper to investigate the VOC measurement capability of Airtrak. This work is based on our considerable experience with photochemical flow reactor experiments carried out with the Airtrak (*8*). First, model simulations of Airtrak experiments were performed to derive relationships between a measurable quantity, i.e., "smog" concentrations, and sample VOC concentrations. Using these relationships, model calculations were performed to simulate ambient VOC measurements. Finally, a preliminary investigation of the implementation of the present methodology to Airtrak was carried out.

Airtrak Flow-Mode Simulations: SP−VOC Relationships

The Airtrak operates by dividing the air sample into three pairs of streams. Streams A are analyzed for NO and NO_y (NO_x + gas-phase oxidation products of NO_x); streams B are used to determine smog and ozone concentrations; and streams C, with excess NO added, are used to determine the smog formation rate coefficient of VOC. Since the C stream measurements of smog produced (SP) with ambient airstreams by Airtrak are similar to flow-mode reactivity experiments (*8*), the relationships of SP to VOC are derived by modeling flow-mode experiments.

Flow-Mode Experiments. In the flow-mode runs used to determine VOC reactivities (*8*), clean air in stream C is mixed continuously with known amounts of NO and VOC mixtures and then divided into streams C1 and C2. Stream C1 passes through a dark (reference) reactor, and stream C2 passes through the photolytic reactor. The reactors are made of Teflon. The volume of both reactors is 10 L, and the flow rate is set at 0.85 L min^{-1}; consequently, the dilution rate in the reactors is 0.085 min^{-1}, and the residence time is approximately 12 min. Temperature in the chambers is maintained at 313 K. The outflow of each reactor passes to a Teflon titration chamber reactor where any ozone formed in the photolytic reactor reacts with the excess NO to produce NO_2. The outflows then pass to the NO analyzer. The difference in NO concentrations between C1 and C2 outflows provides SP in the photolytic reactor:

* Correspondence may be sent to either author; e-mail: tchang@ford.com, sjapar@ford.com; fax: 313-594-2923.

S0013-936X(97)00913-9 CCC: $15.00
Published on Web 06/05/1998

TABLE 1. Chamber-Dependent Parameters Used in Model Simulations of the Airtrak Flow-Mode Experiments

parameter	values	comments
light source		
light intensity, k_1	0.25−0.70 min^{-1}	based on measurements
spectral distribution	one measurement	used for all runs
radical source		
$k(h\nu \rightarrow OH)$	pk_1 (ppm min^{-1})	$p = 1. \times 10^{-4}$−$1. \times 10^{-5}$ ppm
NO_x offgassing		
$k(h\nu \rightarrow NO_2)$	$(1.0 \times 10^{-4}$ ppm$)k_1$	assumed
wall losses		
$k(O3 \rightarrow)$	2.5×10^{-3} min^{-1}	assumed
$k(N_2O_5 \rightarrow)$	2.8×10^{-3} min^{-1}	assumed
$k(NO_2 \rightarrow 0.5\ HONO)$	5.0×10^{-3} min^{-1}	see text
effect of background VOC		
$k(OH \rightarrow HO_2)$	250 min^{-1}	assumed
other parameters		
dilution rate	0.085 min^{-1}	measured
temperature	313 K	maintained for all runs
H_2O concn	2000, 20000 ppm	assumed

$$[SP]_t = [O_3]_t - [O_3]_0 + [NO]_0 - [NO]_t \quad (1)$$

where $[O_3]_t$ and $[NO]_t$ denote concentrations in the photolytic reactor at time t and $[O_3]_0$ and $[NO]_0$ represent the reference concentrations in the dark reactor. In the irradiation chamber, the photochemical steady state is attained in approximately 100 min when VOC and NO_x concentrations in C streams are constant.

Simulation Conditions. To simulate photochemical reactions in the reactor, the SAPRC93 chemical mechanism (*10*), an updated version of the SAPRC90 mechanism (*11*), is used. Representations of chamber effects are needed for the simulations: intensity and spectral distribution of light sources for the calculation of photolysis coefficients of photolyzing species; wall reactions representing radical sources, off-gassing or wall deposition of species. The parameters used in the simulations to represent the chamber-dependent processes are summarized in Table 1. These parameters were measured or assumed based on other chamber measurements (*12*). Values for wall-loss rates for O_3 and NO_2 are higher than those for conventional chambers (*12*) and are based on the reactivity experiments involving NO_2 (see below).

Black lights are used in the Airtrak experiments. The measured NO_2 photolysis rate coefficient k_1 was found to lie in the range of 0.25−0.70 min^{-1} (*8*). The measured relative spectral distribution along with the absorption cross sections and quantum yields for NO_2 and other photolyzing species are used to calculate the ratios of photolysis rate coefficients of all other photolyzing species relative to that of NO_2. A chamber OH source (ppm min^{-1}) is represented by

$$k(h\nu \rightarrow OH) = pk_1 \quad (2)$$

where the parameter p (in ppm) is related to the chamber reactivity. Water vapor concentrations are assumed to be 2000 ppm for dry air experiments and 20 000 ppm for ambient air simulations.

In the present simulations, a VOC mixture (called 9-VOC) and propene are used to derive SP−VOC relationships. The 9-VOC mixture consists of nine components used as an urban surrogate VOC mixture (*8*). VOC species and carbon fractions of the 9-VOC are as follows: *n*-butane, 0.207; 2,3-dimethylpentane, 0.352; ethene, 0.045; propene, 0.058; isobutene, 0.082; *trans*-2-butene, 0.033; toluene, 0.087; *m*-xylene, 0.085; and 1,3,5-trimethylbenzene, 0.049.

For model simulations of flow-mode experiments, gas mixtures in the chambers are assumed to be homogeneous. Reactant source terms corresponding to reactant input are added to the SAPRC93 mechanism in order to simulate flow-mode runs. Source S_i for species i is related to the steady-state concentration C_i without reactions (in the dark chamber):

$$S_i = C_i k_d \quad (3)$$

where k_d is the dilution rate. In Airtrak flow-mode experiments, ozone and other product concentrations are low since the residence time is 12 min and relatively high NO concentrations are maintained in the reaction chamber. The chemistries of all nine species of the 9-VOC mixture are represented explicitly without lumping in the SAPRC93 mechanism. The photochemical steady-state SP concentrations are used to derive SP−VOC relationships in the present section.

Effects of NO and NO_2 on SP. SP concentrations measured by flow-mode experiments are a function of VOC concentrations, VOC composition, NO_x concentrations, reactor temperature, and other variables included in Table 1. In the original development of Airtrak, it had been assumed that [SP] was independent of NO_x concentrations and was directly proportional to VOC concentrations of a given VOC mixture based on the IER model (*6*, *7*):

$$[SP] = KR_i = Ka_i[VOC_i] = A_i[VOC_i] \quad (4)$$

where K is dependent on light intensity, temperature, and residence time of the reactor; R_i is the reactivity-adjusted concentration of mixture VOC_i; a_i is the activity coefficient; and A_i may be called the reactivity coefficient.

However, [SP] is dependent on NO and NO_2 concentrations. In Figure 1, measured and model-calculated [SP] for $[9\text{-VOC}]_0 = 1.0$ and 2.1 ppm C under the steady-state conditions are plotted against NO concentrations (in the reference chamber), $[NO]_0$. As $[NO]_0$ increases, [SP] decreases initially, attains a minimum, and increases again. The value of $[NO]_0$ at which [SP] attains a minimum depends on values of $[NO]_0$ and $[VOC]_0$. The existence of an SP minimum is due to the fact that, as $[NO]_0$ increases, the photochemical oxidation rate of NO decreases while the nonphotochemical oxidation rate of NO increases gradually.

In Figure 2, measured and model-simulated, steady-state [SP] is plotted against varying amounts of NO_2 added for the case of $[NO]_0 = 0.3$ ppm, $[9\text{-VOC}]_0 = 2.1$ ppm C, and different

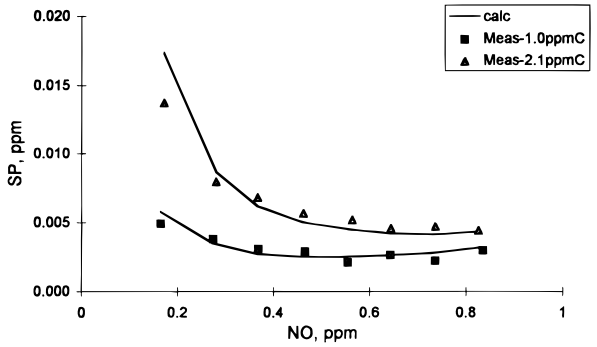

FIGURE 1. Measured and model-calculated steady-state SP vs NO. For the model calculation, $k_1 = 0.29$ min^{-1}, $p = 6.0 \times 10^{-5}$ ppm.

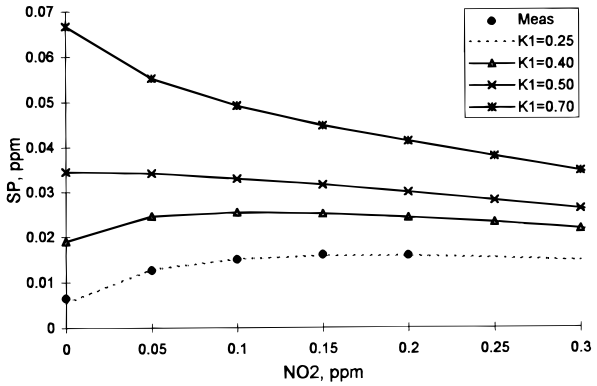

FIGURE 2. Model-calculated steady-state SP vs NO_2. $[NO]_0 = 0.3$ ppm for all cases; $[NO_2]_0$ are varied from 0 to 0.30 ppm; $k_1 = 0.25$, 0.4, 0.5, and 0.7 min^{-1}; and $p = 6.0 \times 10^{-5}$ ppm. For $k_1 = 0.25$ min^{-1}, measured SP are also shown.

k_1 values. The effect of NO_2 was measured near the end of our experimental reactivity program (*8*); consequently, the light intensity was low, i.e., $k_1 = 0.25$ min^{-1}. Measured, steady-state [SP] increases initially and levels off as the added amount of NO_2 increases. This promotional effect on smog formation is surprising since, in conventional chambers, NO_2 inhibits smog formation (*9*, *10*). The photolytic reactor is much smaller than conventional smog chambers. To simulate the NO_2 promotion effect, it was necessary to use higher values for the NO_2 wall-loss rate and the HONO formation rate, as given in Table 1. Model simulations were also carried out for higher values of k_1, and the results are shown in Figure 2. In this case, the NO_2 inhibition effect on smog formation is predominant. Figures 1 and 2 show that SP is quite sensitive to NO_x.

In the Airtrak experiments, the temperature was controlled, and light intensity decayed slowly over the duration of the experimental program. In streams C1 and C2, $[NO]_0$ in the reference chamber can be kept constant by a feedback control. That is, depending on ambient NO and O_3 concentrations that are measured through streams A and B, the flow rate of the excess reagent NO can be controlled to keep $[NO]_0$ constant in the reference chamber. When ambient samples are drawn into the reactors, significant concentrations of NO_2 will exist in the reactors resulting from ambient NO_2 and the reaction of O_3 and the excess reagent NO. Since [SP] is sensitive to NO_2 concentrations (Figure 2), the derivation of SP−VOC relationships must include the effect of NO_2. An alternative approach is to remove O_3 and NO_2 before VOC measurements in ambient air samples (see below).

SP−VOC Relationship. Under the assumption that chamber properties (temperature, wall effects, and light intensity) are fixed and $[NO]_0$ is kept constant, we can investigate the relationship of [SP] to [VOC]. The functional form should be simple so that parameters in the functional representation can be determined relatively easily from the Airtrak flow-mode experiments. First, SP−VOC relationships for the case of $[NO_2]_0 = 0$ are derived. Both the 9-VOC mixture and propene are used as surrogates for VOC. An examination of the flow-mode run data (*8*) and photochemical modeling evaluations shows that, for VOC−NO mixtures with no NO_2 added, steady-state SP can be represented by a quadratic polynomial of VOC concentrations:

$$[SP] = a + b[VOC]_0 + c[VOC]_0^2 \qquad (5)$$

where $[VOC]_0$ is the inlet (or reference) VOC concentration. To derive the parameters in eq 5, [SP] was calculated using the SAPRC93 mechanism and chamber parameters in Table 1 for the range of $[VOC]_0 = 0.1-2$ (interval, 0.1) ppm C for the 9-VOC mixture and 0.05−1 (interval, 0.05) ppm C for propene. $[NO]_0$ is taken to be 0.3 ppm. Parameters ($a-c$) determined by the linear least-squares method are shown in Table 2. Values of the parameters are dependent upon k_1, the VOC composition, and the ranges of VOC concentrations considered. In general, the resulting correlation coefficients are close to 1. For this case, only three parameters need to be determined. This simple approach is applicable to ambient air if NO_2 and O_3 can be removed from the ambient sample without affecting VOC.

TABLE 2. Parameters in eq 5 Determined by the Least-Squares Method[a]

VOC	k_1 (min^{-1})	a	b	c	R^2
9-VOC	0.7	0.0006	0.0096	0.012	0.9997
	0.35	0.0008	0.0016	0.002	0.9992
propene	0.7	−0.0001	0.026	0.059	0.9995
	0.35	0.0014	−0.0005	0.019	0.998

[a] Used $[NO]_0 = 0.3$ ppm, $[H_2O] = 20000$ ppm, $p = 6.0 \times 10^{-5}$ ppm, and other chamber parameters in Table 1.

The effect of NO_2 on SP−VOC relationships has also been investigated. We start from an approximate relationship between [SP] and total peroxy radical concentration $[XO_2]$, derived in Appendix A. Under the NO-rich condition in the Airtrak flow-mode operation, the steady-state [SP] is approximately related to $[XO_2]$:

$$[SP] = [NO]_0 - [NO] = [NO]_0 \frac{k_{XO_2}[XO_2]}{k_d} \qquad (6)$$

where $k_{XO_2}[XO_2]$ represents the sum over all species of peroxy radicals. The steady-state $[XO_2]$ is related to [VOC], $[NO_x]$, and [OH], while [OH] is dependent on [VOC], $[NO_2]$, and light intensity. After examining these steady-state relationships and preliminary modeling results, the following functional form has been chosen:

$$[SP] = \frac{[SP]_0}{1 + \alpha\left(\frac{[NO_2]_0^2}{[VOC]_0}\right)^{\beta}} \qquad (7)$$

where $[VOC]_0$ and $[NO_2]_0$ are inlet (or reference) concentrations of VOC and NO_2, and $[SP]_0$ represents [SP] for the case of $[NO_2]_0 = 0$ given by eq 5. To derive the parameters in eq 7, [SP] was calculated using the SAPRC93 mechanism and chamber parameters in Table 1 for the range of $[VOC]_0 = 0.1-2.0$ (interval, 0.1) ppm C for 9-VOC and $[NO_2] = 0-0.2$ (interval, 0.1) ppm. Regression results show that eq 7

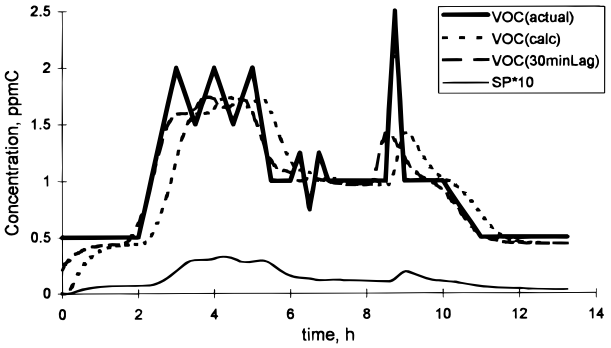

FIGURE 3. Model simulation of VOC measurements for the case of 9-VOC. VOC(actual) is the inlet concentration of 9-VOC, VOC(calc) is derived using model-calculated SP and eq 5 (and Table 2), VOC-(30 min lag) is VOC(calc) transferred backward by 30 min, and $k_1 = 0.7$ min^{-1}.

represents SP quite well in the domain where NO_2 inhibits smog formation. However, eq 7 is too complex to be adapted to the Airtrak. In addition, the Airtrak flow-mode experiments, as discussed above, show that NO_2 can promote smog formation when light intensity is low.

Removal of O_3 and NO_2. To apply the simple SP−VOC relationship (eq 5) for ambient VOC measurements, ozone and NO_2 need to be removed from ambient air samples while leaving VOC unperturbed. Ozone removal techniques relevant to the sampling of atmospheric VOC have been recently reviewed by Helmig (*13*). Numerous ozone removal techniques have been applied. Some of the more universal methods for the VOC sampling include sodium sulfite and sodium thiosulfate. The use of MnO_2 screens appears to be another promising ozone removal technique. Activated MnO_2 has also been shown to remove NO_2 efficiently from ambient air samples (*14*). Triethanolamine and phenoxazene could be used to remove ozone and NO_2 (*15*). However, the effects of these compounds on VOC species have not been investigated sufficiently. Particularly, the effects of specific techniques on oxygenates, including carbonyls, need to be determined.

Simulation of VOC Measurements

In this section, the feasibility of making VOC measurements by the Airtrak is investigated by simulating ambient VOC measurements using the SP−VOC relationship (eq 5) derived above. To simulate ambient situations, temporally varying concentrations of VOC are introduced into the photolytic chamber and the temporal variation of SP concentration in the photolytic chamber is calculated. Using model-calculated [SP], [VOC] is derived using eq 5. If [VOC] derived from [SP] is related quantitatively to inlet VOC concentrations, VOC measurements are feasible. The 9-VOC mixture is taken as the inlet VOC for the present study.

Inlet 9-VOC (representing an ambient sample with O_3 and NO_2 removed) is varied in the range of 0.5−2.5 ppm C. In Figure 3, inlet 9-VOC is shown as VOC(actual), and the temporal variation is represented by the triangular wave for the case of $k_1 = 0.7$ min^{-1}. The inlet VOC concentration is low for the first 2 h, high for the 3−5 h period (to simulate urban rush hours), shows a finer temporal variation for the seventh hour, exhibits a sharp peak for the ninth hour (to simulate a VOC plume), and then decreases gradually for the 9−13 h period.

Model-calculated [SP], which simulates the Airtrak measurement of SP, is also shown in Figure 3. From model-calculated [SP], 9-VOC concentrations are derived using eq 5 with the parameters given in Table 2. Derived 9-VOC concentrations are shown as VOC(calc) in Figure 3. Since response time characteristic of the photolytic reactor is

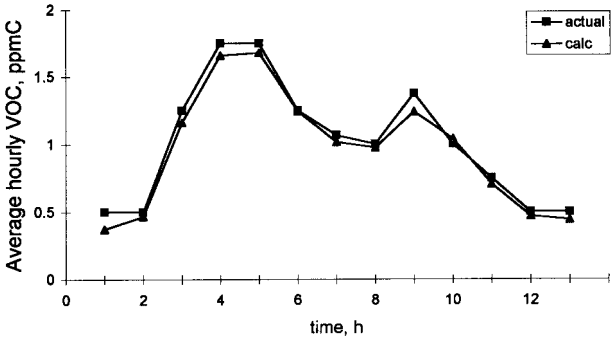

FIGURE 4. Average hourly concentrations of actual inlet 9-VOC and model-calculated 9-VOC as a function of time based on results of Figure 3.

approximately 30 min, it is assumed that the derived 9-VOC concentration at time t corresponds to VOC concentration at $(t - 30)$ min and is shown as VOC(30 min lag) in Figure 3. VOC(30 min lag) corresponds to the measured VOC and represents the temporal variation of the inlet VOC reasonably well. However, sharp features are smoothed out due to the delayed response time and mixing of the inlet VOC in the photolytic chamber. In addition, the SP−VOC relationships derived in the previous section are based on steady-state [SP], but [SP] in ambient VOC simulations are not truly related to the steady-state situations; consequently, an additional approximation is introduced to the VOC measurement simulations.

For the purpose of air quality modeling and derivation of SP−VOC relationships, average hourly VOC concentrations are usually needed. In Figure 4, average hourly VOC concentrations of inlet 9-VOC and model-calculated 9-VOC are shown. Differences between model-calculated and "actual" 9-VOC are within 5% except for hours 3 and 9. During hours 3 and 9, extreme variations in the actual VOC concentrations are introduced, and differences are about 7%. Such extreme variations of VOC are not likely to occur often in urban and regional areas. Thus, the present simulation demonstrates the feasibility of almost real-time measurements of reactivity-adjusted VOC.

Preliminary Implementation of VOC Measurements to Airtrak

In the previous section, we demonstrated the feasibility of VOC measurements using model simulations. In this section, a preliminary implementation of the methodology to the Airtrak instrument is investigated. First, the feasibility of calibration or determination of model parameters is investigated. Since model parameters in eq 5 are dependent on VOC species, 9-VOC (which is designed as a surrogate urban VOC mixture) is a better choice than propene for instrument calibration for the purpose of ambient VOC measurements. Second, temporally varying amounts of VOC are introduced into the photolytic chamber, and measured VOC are derived from measured SP to show how well measured VOC represent inlet VOC.

VOC−NO Mixture Experiments. An Airtrak run with 9-VOC/NO mixtures is shown in Figure 5, where measured SP (6-min average) and inlet VOC concentrations are shown. For this run, the VOC concentration was varied every 2−3 h; consequently, the steady state for each VOC level was attained. Using steady-state [SP], the following relationship is obtained:

$$[\mathrm{SP}] = 0.0021 + 0.0029[\mathrm{VOC}]_0 + 0.0014[\mathrm{VOC}]_0^2 \quad (8)$$

with correlation coefficient, $R^2 = 0.997$. $[\mathrm{VOC}]_0$ are in ppm, and the constant term represents the background reactivity.

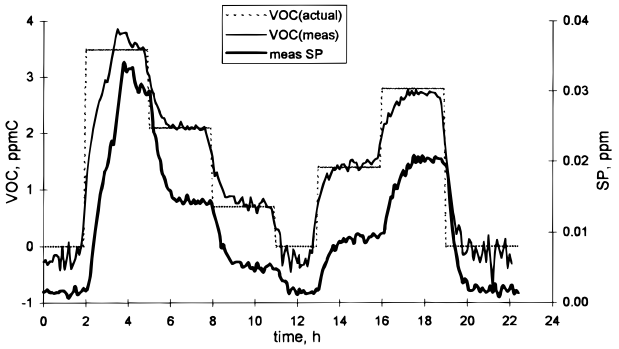

FIGURE 5. Measured SP (6 min average) and VOC concentrations (6 min average) derived from measured SP and eq 8 with 30 min lag. Inlet VOC concentrations of 9-VOC are also shown. Inlet NO concentrations are 0.31 ppm.

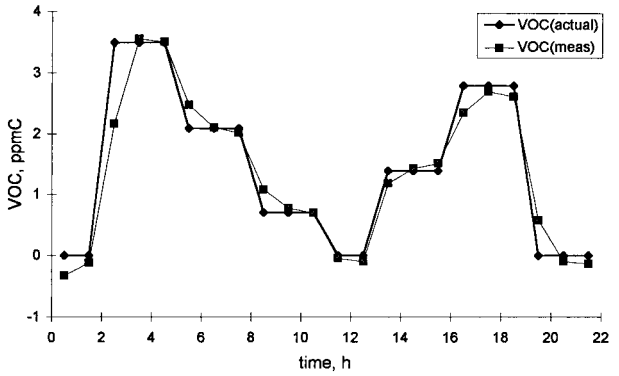

FIGURE 6. Average hourly concentrations of actual inlet VOC and VOC concentrations (with 30 min lag) derived from measured SP.

The values of coefficients in eq 8 are consistent with those of the modeling results in Table 2. In Figure 5, VOC concentrations (6-min average), derived using measured SP and eq 8 with 30 min lag, are also shown. In Figure 6, 1-h average VOC concentrations derived using measured SP and eq 8 with 30 min lag are shown along with 1-h average inlet VOC. The Airtrak-derived VOC represents inlet VOC reasonably well.

A Possible Strategy for Ambient Measurement. To implement the methodology to the Airtrak, two features have to be added: an ambient sampling strategy and a calibration procedure. O_3 and NO_2 have to be removed from ambient air samples by appropriate scrubbers as discussed above. Ambient sampling strategies, particularly involving the removal of NO_2, need to be investigated. To keep the photolytic reactor stable, water vapor may have to be removed from ambient air samples, perhaps using methodology such as used by Goldan et al. (*2*). The reactivity of the reactor walls is shown to be reasonably stable, if VOC concentrations are not excessively high as compared to urban VOC levels (*8*).

To calibrate the Airtrak for VOC measurements or to determine the parameters in eq 5, 9-VOC (which is a surrogate urban VOC mixture) is a better calibration gas than a simple VOC species such as propene, as pointed out above. For measurements in rural areas, a different VOC mixture, which is more representative of the actual ambient, rural VOCs, would be needed for calibration. Several hours are needed to determine all three parameters in eq 5, as shown in the derivation of eq 8. This full calibration could be performed weekly. A simple calibration, which scales the weekly determined calibration function, could be performed daily during predawn hours. This simple daily calibration would take 2 h since a measurement of the steady-state SP for a reference VOC level is needed. All remaining hours could be used for ambient measurements. These calibration and ambient measurement strategies could be automated as demonstrated during our reactivity measurement program (*8*). Thus, semicontinuous measurements of reactivity-adjusted VOC could be possible if the methodology, demonstrated by modeling simulations and preliminary experiments, is implemented properly. However, a more comprehensive study is needed to demonstrate the practicality of the methodology suggested in this paper. Further tests with additional calibration VOC mixtures are needed, and the removal of O_3 and NO_2 from air samples has to be demonstrated.

Appendix A: SP—Peroxy Radical Relationship under the Steady-State Conditions

Under the NO-rich conditions in the Airtrak flow-mode operation, the rate equations for [NO] and [O_3] in the photolytic chamber can be expressed as

$$\frac{d[O_3]}{dt} = k_1[NO_2] - k_3[O_3][NO] - k_d[O_3] \qquad (A1)$$

$$\frac{d[NO]}{dt} = k_1[NO_2] - k_3[O_3][NO] - k_{XO_2}[XO_2][NO] + k_d([NO]_0 - [NO]) \qquad (A2)$$

where k_1 is the photolysis rate coefficient for NO_2, k_3 is the rate constant for NO + O_3 reaction, k_d is the dilution rate, k_{XO_2} represents the rate constant for NO + XO_2 reaction, XO_2 represents peroxy radicals, and $[NO]_0$ represents the reference NO concentration in the reference chamber. The term $k_{XO_2}[XO_2]$ in eq A2 represents the sum over all species of peroxy radicals, $\Sigma k_{XO_2i}[XO_2i]$. Under the NO-rich condition, $k_d[O_3]$ can be neglected as compared to $k_3[O_3][NO]$, and the following equation is obtained from eqs A1 and A2:

$$\frac{d([O_3] - [NO])}{dt} = k_{XO_2}[XO_2][NO] - k_d([NO]_0 - [NO]) \qquad (A3)$$

Under the steady-state condition, the NO concentration is obtained from eq A3:

$$[NO] = \frac{k_d[NO]_0}{k_d + k_{XO_2}[XO_2]} \qquad (A4)$$

Under the NO-rich condition, [O_3] is much lower than [NO] and the SP can be approximated by

$$[SP] = [NO]_0 - [NO] = [NO]_0 \frac{k_{XO_2}[XO_2]}{k_d + k_{XO_2}[XO_2]} \qquad (A5)$$

Under the Airtrak operation, k_d is much larger than $k_{XO_2}(XO_2)$ for a wide range of experimental conditions. Consequently, the steady state [SP] can be approximated by

$$[SP] = [NO]_0 - [NO] = [NO]_0 \frac{k_{XO_2}[XO_2]}{k_d} \qquad (A6)$$

Model simulation results using the SAPRC93 mechanism show that eqs A5 and A6 hold approximately for a wide range of experimental conditions. Equations A5 and A6 show that, by measuring [SP], gross (k_{XO_2}-weighted) peroxy radical concentrations can be derived.

Literature Cited

(1) *Rethinking the Ozone Problem in Urban and Regional Air Pollution*; National Research Council, National Academy Press: Washington, DC, 1991.

(2) Goldan, P. D.; Kuster, W. C.; Fehsenfeld, F. C. *J. Geophys. Res.* **1995**, *D100*, 25945−25963.
(3) Romanovsky, J. C.; Taylor, J. R.; MacPhee, R. D.; Dickinson, J. E. Air monitoring of Los Angeles atmosphere with automatic instruments. *Proceedings of 49th Annual Meeting of APCA*; Air & Waste Management Association: Pittsburgh, PA, 1956.
(4) Ortman, G. C. *ISA Trans.* **1982**, *21*, 15−28.
(5) Belanger, E. B.; Ortman, G. C. *Atmos. Environ.* **1984**, *18*, 1447−1452.
(6) Johnson, G. M.; Quigley, S. M. A universal monitor for photochemical smog. *82nd Annual Meeting of Air & Waste Management Association*; Air & Waste Management Association: Pittsburgh, PA, 1989; Paper No. 89-29.8.
(7) Johnson, G. M. A simple model for predicting the ozone concentration of ambient air. *Proceedings of the Eighth International Clean Air Conference*, Melbourne, Australia, 1984.
(8) Hurley, M. D.; Chang, T. Y.; Wallington, T. J.; Japar, S. M. *Environ. Sci. Technol.* **1998**, *32*, 1913−1919.
(9) Kelly, N. A.; Wang, P. Comparison between smog chamber measurements and theoretical predictions of reactivity. *89th Annual Meeting of Air & Waste Management Association*; Air & Waste Management Association: Pittsburgh, PA, 1996; Paper No. 96-WP62B.01.
(10) Carter, W. P. L. *Atmos. Environ.* **1995**, *29*, 2513−2527.
(11) Carter, W. P. L. *Atmos. Environ.* **1990**, *24A*, 481−518.
(12) Carter, W. P. L.; Lurmann, F. L. *Atmos. Environ.* **1991**, *25A*, 2771−2806.
(13) Helmig, D. *Atmos. Environ.* **1997**, *31*, 3635−3651.
(14) Adams, K. M.; Japar, S. M.; Pierson, W. R. *Atmos. Environ.* **1986**, *20*, 1211−1215.
(15) Williams, E. L., II; Grosjean, D. *Environ. Sci. Technol.* **1990**, *24*, 811−814.

Received for review October 17, 1997. Revised manuscript received May 1, 1998. Accepted May 5, 1998.

ES9709132